

Reaching Fractional Quantum Hall States with Optical Flux Lattices

Nigel R. Cooper¹ and Jean Dalibard^{2,3}

¹*T.C.M. Group, Cavendish Laboratory, J. J. Thomson Avenue, Cambridge CB3 0HE, United Kingdom*

²*Laboratoire Kastler Brossel, CNRS, UPMC, ENS, 24 rue Lhomond, F-75005 Paris, France*

³*Collège de France, 11, place Marcelin Berthelot, 75005 Paris, France*

(Dated: 14 December 2012)

We present a robust scheme by which fractional quantum Hall states of bosons can be achieved for ultracold atomic gases. We describe a new form of optical flux lattice, suitable for commonly used atomic species with groundstate angular momentum $J_g = 1$, for which the lowest energy band is topological and nearly dispersionless. Through exact diagonalization studies, we show that, even for moderate interactions, the many-body groundstates consist of bosonic fractional quantum Hall states, including the Laughlin state and the Moore-Read (Pfaffian) state. Under realistic conditions, these phases are shown to have energy gaps that are larger than temperature scales achievable in ultracold gases.

PACS numbers:

There is intense interest in finding new settings in which topological phases of matter analogous to fractional quantum Hall (FQH) states appear. Ultracold atomic gases are ideal systems with which to achieve this goal: they allow studies of strong correlation phenomena for both fermions and bosons, and FQH physics can be approached for homogeneous fluids [1] as well as for atoms confined in optical lattices [2].

While existing theories of FQH-like phases in lattices have focussed on tight-binding models [3–9], one of the most promising routes to topological flat bands for ultracold atoms is through optical flux lattices (OFLs) [10–12]. An OFL uses a set of laser beams to produce a spatially periodic atom-laser coupling that induces resonant transitions between two (or more) internal atomic states. The resulting energy bands, in particular the lowest one, have non-zero Chern numbers, and can be made narrow in energy [12]. This opens the path to experimental studies of novel strong correlation phenomena in topological flat bands, notably the FQH effect of bosons.

We present in this paper the first characterization of the many-body ground state of bosons in an OFL. We start with the design of a novel type of OFL, which fully exploits the structure of the most commonly used (bosonic) atomic species. The scheme is robust since, by contrast to some other OFL proposals [10], it does not require phase locking between the various optical beams composing the lattice. For optimized parameters its lowest band has Chern number 1 and is nearly dispersionless, closely analogous to the lowest Landau level for charged particles moving in a uniform magnetic field. We use exact diagonalization to determine the many-body spectrum of a bosonic gas in this OFL. We show that FQH ground states appear for relatively weak atom interaction at the same filling factors as for a continuum Landau level [1]. Our work provides a concrete experimental scheme by which FQH states of bosons can be realized with large energy scales. Furthermore, it provides the first example of a non-Abelian quantum Hall state (the $\nu = 1$ Moore-

Read state [13]) in a lattice model at high particle density with only two-body interactions.

We focus in this paper on the case of atoms whose internal ground level has angular momentum $J_g = 1$. This is the case for several stable bosonic isotopes of alkali metal species, namely ^7Li , ^{23}Na , ^{39}K , ^{41}K , ^{87}Rb . We denote $|X\rangle$, $|Y\rangle$, $|Z\rangle$ a basis of this level, defined such that $\hat{J}_X|X\rangle = 0$ (and similarly for Y and Z). Here the set of directions X, Y, Z represents an orthogonal trihedron of the physical space [see Figure 1(a)] and \hat{J}_X stands for the component of the angular momentum operator along the X direction. Note that one can replace $|X\rangle$, $|Y\rangle$, $|Z\rangle$ by a triplet of internal states selected among a more complex level scheme, as proposed *e.g.* in [14]. Our scheme will apply as long as each pair of states can be coupled by a resonant two-photon Raman transition with a negligible spontaneous emission rate [15].

We assume that $|X\rangle$, $|Y\rangle$, $|Z\rangle$ are the eigenstates of the atomic Hamiltonian in the absence of atom-laser coupling. We suppose that these three states are non-degenerate and non-equally spaced, and their energies are such that $E_X < E_Y < E_Z$, with $E_Z - E_Y \neq E_Y - E_X$. For alkali atoms this situation can be reached by illuminating the atomic sample with microwaves close to the hyperfine resonance (see supplementary information). We denote by z the $(1, 1, 1)$ direction of the X, Y, Z trihedron, and assume that the centre-of-mass motion of the atoms along the direction z is frozen. Therefore we consider in the following only the atomic motion in the perpendicular xy plane [see Figure 1(a)].

The atoms are irradiated with laser beams propagating in the xy plane along three directions making an angle of $2\pi/3$ with each other. The three wave vectors are $\mathbf{k}_1 = k/2(\sqrt{3}\mathbf{u}_x + \mathbf{u}_y)$, $\mathbf{k}_2 = k/2(-\sqrt{3}\mathbf{u}_x + \mathbf{u}_y)$ and $\mathbf{k}_3 = -k\mathbf{u}_y$, where $\{\mathbf{u}_x, \mathbf{u}_y\}$ is an orthogonal unit basis of the xy plane. Here k stands for the typical wave number of the laser beams [16]. We choose the frequency components in each laser beam so that an atom can undergo resonant Raman transitions between the three internal

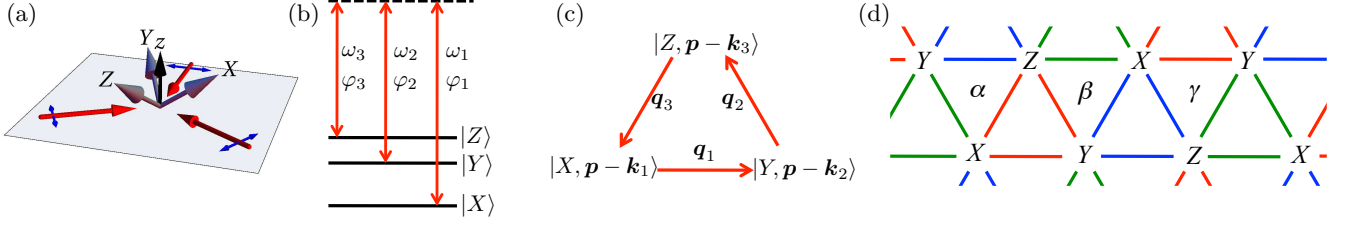


FIG. 1: (a) Atoms with a ground state with angular momentum $J_g = 1$ are irradiated by three laser running waves propagating in the xy plane, whose wave vectors \mathbf{k}_i , $i = 1, 2, 3$ make an angle of $2\pi/3$ with each other. (b) Triplet of light frequencies ω_i ensuring that the three possible Raman transitions are resonantly driven. (c) Graphic representation of three internal+momentum eigenstates, which are resonantly coupled by the laser beams whose frequencies are shown in (b). (d) Infinite array of internal+momentum eigenstates that are resonantly coupled when three triplets of frequencies ω_i (red), ω'_i (green), ω''_i (blue) are simultaneously applied (see also Table I).

states, by absorbing a photon in one wave and emitting a photon in a stimulated manner in another wave. The momentum change in such a transition is $\pm \mathbf{q}_i$, where $\mathbf{q}_i = \mathbf{k}_i - \mathbf{k}_{i+1}$. Here we set $\mathbf{k}_4 \equiv \mathbf{k}_1$ and take $\hbar = 1$ for simplicity.

Suppose first that each beam i consists only of a monochromatic plane wave with frequency ω_i and phase φ_i , and that the ω_i 's are chosen such the three Raman conditions are fulfilled: $\omega_1 - \omega_2 = E_Y - E_X$, $\omega_2 - \omega_3 = E_Z - E_Y$ [and thus $\omega_1 - \omega_3 = E_Z - E_X$, see Figure 1(b)]. Each family of momentum eigenstates $\mathcal{F}(\mathbf{p}) = \{ |X, \mathbf{p} - \mathbf{k}_1\rangle, |Y, \mathbf{p} - \mathbf{k}_2\rangle, |Z, \mathbf{p} - \mathbf{k}_3\rangle \}$ generates a manifold that is globally stable with respect to atom-laser coupling. The three states of $\mathcal{F}(\mathbf{p})$ form an equilateral triangle in momentum space [Figure 1(c)]. The coupling between the atom and the laser field can be written (see supplementary material)

$$\hat{V} = -\Omega \left(|Y\rangle\langle X| e^{i(\mathbf{q}_1 \cdot \mathbf{r} + \varphi_1 - \varphi_2)} + |Z\rangle\langle Y| e^{i(\mathbf{q}_2 \cdot \mathbf{r} + \varphi_2 - \varphi_3)} + |X\rangle\langle Z| e^{i(\mathbf{q}_3 \cdot \mathbf{r} + \varphi_3 - \varphi_1)} \right) + \text{H.c.}, \quad (1)$$

where H.c. stands for Hermitian conjugate. The amplitude and sign of the coupling strength Ω can be adjusted by tuning the intensity of the coupling lasers, and their detuning with respect to the atomic resonance. The fact that all three Raman transitions in Eq. (1) have the same amplitude is ensured by (i) taking the same intensity for each laser beam, (ii) choosing in-plane linear polarizations. A similar ring-coupling scheme has been used in [17] to implement the Peierls substitution in a 1D optical lattice. However in [17] only two laser Raman transitions were used and the ring was closed using radio frequency transitions, which is not appropriate for our purpose.

With only one triplet of laser frequencies as in Fig. 1(b), we do not produce the desired infinite periodic lattice for the atomic motion in momentum space [12]. However this goal can be reached by adding inside the beams i two other triplets of frequency components ω'_i and ω''_i , $i = 1, 2, 3$. Here the roles are circularly exchanged with respect to the first triplet ω_i : The

	$X \rightarrow Y$	$Y \rightarrow Z$	$Z \rightarrow X$
\mathbf{q}_1	$e^{i(\varphi_1 - \varphi_2)}$	$e^{i(\varphi'_1 - \varphi'_2)}$	$e^{i(\varphi''_1 - \varphi''_2)}$
\mathbf{q}_2	$e^{i(\varphi'_2 - \varphi'_3)}$	$e^{i(\varphi_2 - \varphi_3)}$	$e^{i(\varphi''_2 - \varphi''_3)}$
\mathbf{q}_3	$e^{i(\varphi''_3 - \varphi''_1)}$	$e^{i(\varphi'_3 - \varphi'_1)}$	$e^{i(\varphi_3 - \varphi_1)}$

TABLE I: Phases of the Raman coupling matrix elements. Each line corresponds to a given momentum kick $\mathbf{q}_i = \mathbf{k}_i - \mathbf{k}_{i+1}$, and each column to a given pair of internal atomic states. This 3×3 array can be understood as a determinant: each of the six terms appearing in the calculation of this determinant corresponds to one of the six types of triangles in Fig. 1(d). The terms with positive (resp. negative) sign in the determinant calculation are for the upwards (resp. downwards) pointing triangles.

ω'_i (resp. ω''_i) are such that $\omega'_2 - \omega'_3 = E_Y - E_X$ and $\omega'_3 - \omega'_1 = E_Z - E_Y$ (resp. $\omega''_3 - \omega''_1 = E_Y - E_X$ and $\omega''_1 - \omega''_2 = E_Z - E_Y$). In the following we suppose that the differences between the average frequencies $\bar{\omega}, \bar{\omega}', \bar{\omega}''$ of the triplets are much larger than the splittings $E_\alpha - E_\beta$. Processes involving the absorption of a photon from a frequency triplet and the stimulated emission of a photon in another triplet thus play a negligible role.

With the three frequency triplets acting simultaneously on an atom, the family of states that are coupled to a given initial state can be represented by the infinite lattice in momentum space shown in Fig. 1(d). Since there are 3 possible Raman transitions and 3 possible pairs of beams to induce a given transition, the atom-laser coupling \hat{V} generalizing (1) is now characterized by 9 matrix elements. These elements depend on the 9 phases $\varphi_i, \varphi'_i, \varphi''_i$ and are summarized in Table 1. From this Table, it is straightforward to write down explicitly the coupling \hat{V} . For example the three terms appearing in (1) correspond to the diagonal terms of the array of Table I.

In order to characterize the possible non-trivial topology associated with the lattice in momentum space, we now evaluate the total phase gained by an atom when it undergoes a series of Raman transitions $X \rightarrow Y \rightarrow$

$Z \rightarrow X$ and performs a closed loop in momentum space. This corresponds to traveling around the three sides of one of the triangles of Fig. 1(d). The resulting phase is different for upwards pointing triangles [such as the one of Fig. 1(c)] and downwards pointing ones [like the triangles labelled α, β, γ in Fig. 1(d)]. For an upwards pointing triangle, the global phase is always zero. Indeed moving around the sides of such a triangle involves absorption and stimulated emission of photons whose frequencies belong to the same triplet, *e.g.* the ω_i triplet for the triangle of Fig. 1(c). Therefore each laser phase φ_i (or φ'_i, φ''_i) enters both with a + and a - sign in the total accumulated phase around such a triangle, leading to a null result.

Downwards pointing triangles on the other hand correspond to a non-trivial phase. Consider for example the clockwise oriented path around the sides of the triangle labelled α in Fig. 1(d): (i) The $X \rightarrow Y$ transition is accompanied by a change of atomic momentum \mathbf{q}_2 , and it corresponds to a phase change $\varphi'_2 - \varphi'_3$ (see Table I); (ii) the $Y \rightarrow Z$ transition is along \mathbf{q}_1 , with the phase change $\varphi''_1 - \varphi''_2$; (iii) the $Z \rightarrow X$ transition is along \mathbf{q}_3 , with the phase change $\varphi_3 - \varphi_1$. As a result, the phase accumulated when traveling around the sides of triangle α is

$$\Phi_\alpha = \varphi''_1 - \varphi_1 + \varphi'_2 - \varphi''_2 + \varphi_3 - \varphi'_3. \quad (2)$$

We can similarly calculate the phases $\Phi_{\beta, \gamma}$ for the two other downwards pointing triangles. Although the sum $\Phi_\alpha + \Phi_\beta + \Phi_\gamma$ is always zero, we can identify configurations such that each of these three phases takes a non-trivial value. For example the choice $\varphi_1 = 2\pi/3$, $\varphi_3 = -2\pi/3$, and all other phases equal to zero yields

$$\Phi_\alpha = \Phi_\beta = \Phi_\gamma = 2\pi/3 \pmod{2\pi}. \quad (3)$$

From now on, we will stick to this choice, together with the assumption that $\Omega > 0$, which is obtained for an alkali-metal atom by tuning the lasers between the D_1 and D_2 resonance lines.

The OFL formed in this way has a reciprocal lattice spanned by the basis vectors $\mathbf{G}_1 = 3\mathbf{q}_1$ and $\mathbf{G}_2 = \mathbf{q}_2$. The real space lattice vectors are $\mathbf{a}_1 = \frac{2\pi}{3\sqrt{3}q}(\sqrt{3}\mathbf{u}_x + \mathbf{u}_y)$ and $\mathbf{a}_2 = \frac{4\pi}{\sqrt{3}q}\mathbf{u}_y$, where $q = |\mathbf{q}_i| = \sqrt{3}k$. This geometry is equivalent to that of the three-state triangular flux lattice of Ref. 12. However, the pattern of phases in the reciprocal space tight binding model differs: here we have fluxes of 0 and $2\pi/3$ in the upwards and downwards pointing triangles, as opposed to $\pi/3$ for each [12]. Nevertheless, the physical properties of the OFLs are very similar: in each unit cell of the real space lattice the lowest energy dressed state experiences $N_\phi = 1$ flux quantum; the resulting bandstructure shows low energy bands that are analogous to Landau levels. In particular, the lowest energy band has Chern number of 1, and very narrow energy width, W , over a broad range of lattice depths Ω . Here we focus on a lattice of depth $\Omega = 3E_R$ [where

$E_R \equiv q^2/(2m)$ is the recoil energy for atomic mass m] close to which this bandwidth has a (local) minimum of $W \simeq 0.015E_R$. In view of this very small bandwidth, the system is highly susceptible to the formation of strongly correlated phases even for relatively weak interactions.

We have used exact diagonalization to study the groundstates of interacting bosons occupying the lowest energy band of the OFL for $\Omega = 3E_R$. (We neglect the population of higher bands, since the gap to the next band is very large, $\Delta \simeq 46W$.) We consider the bosons to interact via spin-independent contact interactions, which is a good approximation for ^{87}Rb . We write the two-dimensional coupling constant as $g_{2D} = \frac{\hbar^2}{m}\tilde{g}$, where \tilde{g} is dimensionless. For atoms with 3D scattering length a_s restricted to 2D by a harmonic confinement of oscillator length a_0 , and neglecting (sub)band mixing, this is $\tilde{g} = \sqrt{8\pi}a_s/a_0$ [18]. We study a finite system in a periodic geometry, with sides $\mathbf{L}_1 = N_1\mathbf{a}_1$ and $\mathbf{L}_2 = N_2\mathbf{a}_2$, where $N_{1,2}$ are integers. The total flux is then $N_\phi = N_1N_2$, so for N particles the Landau level filling factor is $\nu \equiv N/N_\phi$. The interacting many-particle states can be classified by a conserved crystal momentum at N_ϕ points in the Brillouin zone. We construct the Hamiltonian at each crystal momentum and use a standard Lanczos method to determine the low energy spectrum.

For very weak interactions, $\tilde{g} \ll 1$, the bosons form a condensate in the minima of the band dispersion. However, our numerical results show that, even for moderate interaction strength $\tilde{g} \gtrsim 0.2$, this (compressible) condensed phase is replaced by strongly correlated (incompressible) FQH states at filling factors $\nu = 1/2, 2/3, 3/4$ and 1. Here, we focus on the FQH states at $\nu = 1/2$ and 1. (Results for $\nu = 2/3, 3/4$ are described in the Supplementary Material.)

Evidence for the appearance of incompressible phases is found by calculating the discontinuity in the chemical potential $\Delta\mu$ for the groundstate: the difference between the chemical potential for adding a particle and that for removing a particle. A non-zero and positive $\Delta\mu$ indicates that the system is incompressible. To minimize finite-size effects we define [19] $\Delta\mu \equiv N[E_{N+1}/(N+1) + E_{N-1}/(N-1) - 2E_N/N]$, where E_N is the groundstate energy for N particles.

In Fig. 2 we plot the dependence of $\Delta\mu$ on interaction strength \tilde{g} at filling factors $\nu = 1/2$ and 1. For $\nu = 1/2$ there is an onset of incompressibility for $\tilde{g} \gtrsim 0.2$, and for $\nu = 1$ incompressibility appears for $\tilde{g} \gtrsim 0.4$. In the thermodynamic limit, $N \rightarrow \infty$, the transitions from compressible $\Delta\mu = 0$ to incompressible $\Delta\mu > 0$ should be sharp, and can even be discontinuous for first-order transitions, but are rounded in Fig. 2 by finite-size effects. The observed rises of $\Delta\mu$ are indications of the approximate values of \tilde{g} at which there are transitions into the incompressible phases.

To explore the nature of these incompressible phases it

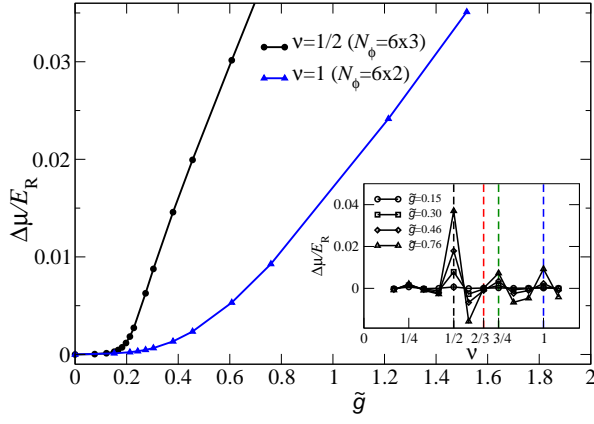


FIG. 2: Incompressibility, as measured by the discontinuity in the chemical potential $\Delta\mu$ defined in the text, as a function of interaction strength \tilde{g} at several filling factors: $\nu = 1/2$ (for $N = 9$ bosons in a system of size $N_\phi = N_1 N_2 = 6 \times 3$, circles); and $\nu = 1$ ($N = 12$ in $N_\phi = 6 \times 2$, triangles). The inset shows $\Delta\mu$ as a function of filling factor for a series of interaction strengths \tilde{g} .

is instructive to study their (neutral) excitation spectra in the strong-interaction limit $\tilde{g} \rightarrow \infty$. These spectra, Fig. 3, show all the expected properties of the bosonic Laughlin ($\nu = 1/2$) and Moore-Read ($\nu = 1$) states. On this periodic geometry, these topologically ordered incompressible phases should show groundstate degeneracies (of 2 and 3 respectively) in the thermodynamic limit, separated by an energy gap from the remaining excitations. As shown in Fig. 3, even for these finite systems these groundstate degeneracies appear clearly. Results on other system sizes and geometries (not shown) are consistent with these results, confirming that these near degeneracies are robust features, not imposed by symmetries, that characterize these topological phases.

The FQH states that we find for the OFL (at $\nu = 1/2, 2/3, 3/4, 1$) are the same as those found for contact interacting bosons in the continuum lowest Landau level (LLL) [1]. We have established the equivalence of the phases of these two models by studying the evolution of the many-body spectrum for a series of Bloch wavefunctions that interpolate between those of the lowest band of the OFL and those of the LLL. To do so, we consider a fictitious atom with $N_s = 12$ internal states, and represent the LLL by the $N_s = 12$ triangular OFL of Ref. 12, the lowest band of which has properties that are indistinguishable from those of the LLL for suitable coupling $\Omega' \simeq 10E_R$ [20]. We place 9 additional internal states at the midpoints of the bonds of Fig.1(d), coupled to each other and to the original states X, Y, Z by bonds of strength Ω' and with $\pi/12$ flux through each new triangular plaquette [21]. Choosing $(\Omega, \Omega') = (3(1 - \lambda), 10\lambda)E_R$ and varying λ leads to smooth interpolation of the lowest energy band and the many-body spectrum, from those of the present model ($\lambda = 0$) to those of the LLL ($\lambda = 1$).

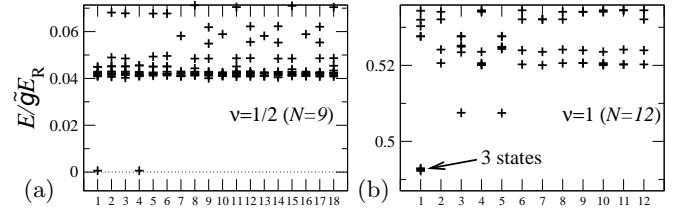


FIG. 3: Low-energy spectra for the OFL with $\Omega/E_R = 3$ in the strong-interaction limit $\tilde{g} \rightarrow \infty$ at filling factors (a) $\nu = 1/2$ ($N = 9$ bosons in $N_\phi = N_1 N_2 = 6 \times 3$) and (b) $\nu = 1$ ($N = 12$ bosons in $N_1 N_2 = 6 \times 2$). The crystal momentum $\mathbf{k} \equiv \alpha_1 \mathbf{G}_1/N_1 + \alpha_2 \mathbf{G}_2/N_2$ is labelled by the index, $i = 1 + \alpha_1 + N_1 \alpha_2$ for $\alpha_1 = 0, \dots, N_1 - 1$ and $\alpha_2 = 0, N_2 - 1$. The quasi-degenerate groundstates have the expected multiplicities and crystal momenta for the Laughlin state ($\nu = 1/2$), and the Moore-Read state ($\nu = 1$).

In all cases ($\nu = 1/2, 2/3, 3/4, 1$) the energy gap remains open, showing that the phases of these two models are the same [22, 23]. Indeed, there is very little change in the spectrum, showing that this OFL (with $\Omega = 3E_R$) is a very close representation of the LLL. For example, for the LLL the $\nu = 1/2$ state has zero interaction energy, as the two-body correlation function vanishes exactly at zero range. Here, the $\nu = 1/2$ state in the OFL has $E_N/N \simeq 7 \times 10^{-5} \tilde{g} E_R$ [see Fig. 3(a)] showing that the zero-range two-body correlation function nearly vanishes.

To summarize we have proposed a robust atom-laser configuration that can lead to FQH states of bosons in a well-accessible range of parameters. The robustness of the setup is ensured by the absence of need for a stabilization of the relative phases of different beams [24]. The only phase difference to be controlled is within each single-mode laser beam ($\varphi_i, \varphi'_i, \varphi''_i$) and can be set by acoustic-optic modulators driven by programmable function generators. The lowest energy band is insensitive to fluctuations in the laser amplitudes around $\Omega = 3E_R$, its bandwidth increasing by less than $10^{-3} E_R$ within the range $\Omega/E_R = 2 - 4$, and its topology remaining unchanged. The minimal interaction strength $\tilde{g} \approx 0.2$ for obtaining FQH states corresponds to a 2D confinement frequency of $\gtrsim 7$ kHz for Rb, which is readily achieved in an optical lattice. A clear signal of the formation of strongly correlated phases would be the appearance of density plateaus (wedding cake structure) in in-situ images of the gas, arising from incompressibility $\Delta\mu > 0$. This requires the temperature to be smaller than $\Delta\mu$, which for the Laughlin state we find from Fig. 2 to be $\approx 0.02 E_R$ for $\tilde{g} = 0.4$, that is 10 nK for ^{87}Rb .

This work was supported by the Royal Society of London, EPSRC Grant EP/J017639/1 (NRC), IFRAF and ANR (Grant AGAFON). We acknowledge useful discussions with J. Beugnon, L. Corman, C. Cohen-Tannoudji, F. Gerbier, G. Möller, and S. Nascimbène.

-
- [1] N. R. Cooper, *Advances in Physics* **57**, 539 (2008).
 - [2] M. Lewenstein *et al.*, *Advances in Physics* **56**, 243 (2007).
 - [3] A. S. Sørensen, E. Demler, and M. D. Lukin, *Phys. Rev. Lett.* **94**, 086803 (2005).
 - [4] G. Möller and N. R. Cooper, *Phys. Rev. Lett.* **103**, 105303 (2009).
 - [5] L. Mazza, M. Rizzi, M. Lewenstein, and J. I. Cirac, *Phys. Rev. A* **82**, 043629 (2010).
 - [6] T. Neupert, L. Santos, C. Chamon, and C. Mudry, *Phys. Rev. Lett.* **106**, 236804 (2011).
 - [7] D. Sheng, Z.-C. Gu, K. Sun, and L. Sheng, *Nat. Commun.* **2**, 389 (2011).
 - [8] N. Regnault and B. A. Bernevig, *Phys. Rev. X* **1**, 021014 (2011).
 - [9] L. Hormozi, G. Möller and S. H. Simon, *Phys. Rev. Lett.* **108**, 256809 (2012).
 - [10] N. R. Cooper, *Phys. Rev. Lett.* **106**, 175301 (2011).
 - [11] N. R. Cooper and J. Dalibard, *Europhysics Letters* **95**, 66004 (2011).
 - [12] N. R. Cooper and R. Moessner, *Phys. Rev. Lett.* **109**, 215302 (2012).
 - [13] G. Moore and N. Read, *Nucl. Phys. B* **360**, 362 (1991).
 - [14] D. L. Campbell, G. Juzeliūnas, and I. B. Spielman, *Phys. Rev. A* **84**, 025602 (2011).
 - [15] The three states $|X\rangle$, $|Y\rangle$, $|Z\rangle$ can also stand for different motional states, such as the first three vibrational states along the strongly confined direction z . However in this case, the hypothesis of a single, state-independent interaction strength should be relaxed.
 - [16] Although these beams do not have exactly the same frequency, the difference between wave numbers is negligible.
 - [17] K. Jiménez-García *et al.*, *Phys. Rev. Lett.* **108**, 225303 (2012).
 - [18] Z. Hadzibabic and J. Dalibard, *Rivista del Nuovo Cimento* **34**, 389 (2011).
 - [19] N. R. Cooper, N. K. Wilkin, and J. M. F. Gunn, *Phys. Rev. Lett.* **87**, 120405 (2001).
 - [20] Deviations from the continuum Landau level fall exponentially with N_s [12], and are negligible for $N_s = 12$.
 - [21] This new model has net flux $\pi/3$ through each triangle of Fig. 1(d). In connecting the new (Ω') bonds to those (Ω) of the original model (with fluxes of 0 and $2\pi/3$ through upwards and downwards pointing triangles), we assign flux $\pi/3$ through the loop formed by the two sets of bonds spanning each link \mathbf{q}_3 .
 - [22] T. Scaffidi and G. Möller, *Phys. Rev. Lett.* **109**, 246805 (2012).
 - [23] Y.-H. Wu, J. K. Jain, and K. Sun, *Phys. Rev. B* **86**, 165129 (2012).
 - [24] This robustness shows up in the evaluation of the phase around the sides of any triangle of Fig. 1(d): each beam i enters both with a positive sign (*i.e.*, absorption) and a negative sign (*i.e.*, stimulated emission), so that its path length cancels out.

Supplementary material

THE BASIS SET $|X\rangle, |Y\rangle, |Z\rangle$

The components \hat{J}_X and \hat{J}_Y of a spin 1 angular momentum operator read in the standard eigenbasis $\{|m_Z = +1\rangle, |m_Z = 0\rangle, |m_Z = -1\rangle\}$ of \hat{J}_Z :

$$\hat{J}_X = \frac{1}{\sqrt{2}} \begin{pmatrix} 0 & 1 & 0 \\ 1 & 0 & 1 \\ 0 & 1 & 0 \end{pmatrix} \quad \hat{J}_Y = \frac{1}{\sqrt{2}} \begin{pmatrix} 0 & -i & 0 \\ i & 0 & -i \\ 0 & i & 0 \end{pmatrix}. \quad (\text{S1})$$

In the standard eigenbasis $|m_Z = 0, \pm 1\rangle$, we define the eigenvectors $|\alpha\rangle$ of \hat{J}_α ($\alpha = X, Y, Z$) with zero eigenvalue:

$$|X\rangle = \frac{1}{\sqrt{2}} \begin{pmatrix} -1 \\ 0 \\ 1 \end{pmatrix} \quad |Y\rangle = \frac{i}{\sqrt{2}} \begin{pmatrix} 1 \\ 0 \\ 1 \end{pmatrix} \quad |Z\rangle = \begin{pmatrix} 0 \\ 1 \\ 0 \end{pmatrix}. \quad (\text{S2})$$

These three states also form an orthonormal basis set (denoted hereafter the Cartesian basis) and are such that

$$\hat{J}_X|Y\rangle = i|Z\rangle, \quad \hat{J}_Y|Z\rangle = i|X\rangle, \quad \hat{J}_Z|X\rangle = i|Y\rangle. \quad (\text{S3})$$

For any real 3-vector \mathbf{u} , the state $u_X|X\rangle + u_Y|Y\rangle + u_Z|Z\rangle$ is the eigenstate of $\mathbf{u} \cdot \hat{\mathbf{J}}$ with eigenvalue 0.

MICROWAVE DRESSING OF A SPIN-1 GROUND STATE

We consider an atom from the alkali-metal family with a nuclear spin $I = 3/2$, so that its ground level is split in two hyperfine levels with angular momentum $F = 1$ and $F = 2$. The atom is irradiated with a linearly polarized microwave (mw), whose frequency is detuned by Δ_{mw} from the frequency ω_{hf} of the $F = 1 \leftrightarrow F = 2$ hyperfine transition. The coupling between the mw and the atom (half-Rabi frequency) is defined by $\kappa_{\text{mw}} = \mu_B B_{\text{mw}}/2$, where μ_B is the Bohr magneton and B_{mw} is the amplitude of the oscillating mw magnetic field. We restrict to the case where $\kappa_{\text{mw}} \ll \Delta_{\text{mw}} \ll \omega_{\text{hf}}$. We can then treat the atom-mw coupling using the rotating wave approximation and evaluate the shifts of the Zeeman states of the $F = 1$ level using second-order perturbation theory. Taking the quantization axis parallel to the polarization axis (Z) of the microwave, the shifts of the states $m_Z = 0, \pm 1$ read [1]

$$\Delta E(m_Z) = \frac{\kappa_{\text{mw}}^2}{\Delta_{\text{mw}}} \left(1 - \frac{m_Z^2}{4} \right). \quad (\text{S4})$$

The action of the mw on the $F = 1$ hyperfine level can thus be described by the operator $\alpha + \beta \hat{J}_Z^2$, where $\beta = -\kappa_{\text{mw}}^2/(4\Delta_{\text{mw}})$.

Suppose now that a second mw, at a different detuning Δ'_{mw} and with a linearly polarization along X , also irradiates the atom. In the perturbative framework used above, the combined action of the two mws is described by the effective Hamiltonian $H_{\text{mw,eff}} = \beta \hat{J}_Z^2 + \beta' \hat{J}_X^2$, up to an additive constant. The eigenstates of $H_{\text{mw,eff}}$ are the states $|X\rangle, |Y\rangle, |Z\rangle$ with the energies $\beta, \beta + \beta', \beta'$, respectively.

To estimate the required value for B_{mw} , we start by noticing that when writing the atom-laser coupling [Eqn (1) of the main text], we only take into account the resonant elements. For example we assume that the atom can undergo a transition $|X\rangle \rightarrow |Y\rangle$ via the absorption of a photon \mathbf{k}_1 and the emission of a photon \mathbf{k}_2 , and we neglect the transitions $|X\rangle \rightarrow |Y\rangle$ occurring via the absorption of \mathbf{k}_2 and emission of \mathbf{k}_1 . This is legitimate when the two-photon coupling Ω is small compared to the energy difference between $|X\rangle, |Y\rangle, |Z\rangle$: $\Omega \ll \beta, \beta'$. We also note that the perturbative approach leading to (S4) is valid only when $\kappa_{\text{mw}} \ll \Delta_{\text{mw}}$. Requiring that the two sides of each strong inequality differ by at least a factor 5, we find $\Omega \lesssim \kappa_{\text{mw}}/100$. Consider as an illustration the case of Rubidium atoms for which the optimal two-photon coupling $\Omega = 3q^2/(2m) = 9k^2/(2m) \approx 2\pi \times 30 \text{ kHz}$. The microwave coupling κ_{mw} has to be $\gtrsim 3 \text{ MHz}$, corresponding to a microwave magnetic field of $\gtrsim 4 \text{ G}$. This is a large, but still realistic value, especially if one uses small resonant loops to increase the value of B_{mw} at the location of the atomic sample.

THE LIGHT-SHIFT OPERATOR FOR AN ALKALI-METAL ATOMIC SCHEME

We consider an atom that is irradiated by a monochromatic laser beam of frequency ω . The light-shift operator \hat{V} gives the restriction of the atom-laser coupling to the ground atomic level g at first order in laser intensity [2]. In the absence of electron and nuclear spins, the ground and excited states that are involved in the resonant transition of an alkali-metal atom have an angular momentum $J_g = 0$ and $J_e = 1$, respectively. The atom-laser coupling can be written

$$\hat{U} = \sum_{\alpha=X,Y,Z} \kappa_\alpha |e, \alpha\rangle \langle g| + \text{H.c.} \quad (\text{S5})$$

$$= \sum_{m=0,\pm 1} \kappa_m |e, m\rangle \langle g| + \text{H.c.} \quad (\text{S6})$$

Here the κ_α , $\alpha = X, Y, Z$, (resp. κ_m , $m = 0, \pm 1$) denote the atom-laser coupling strengths (half-Rabi frequencies) in the Cartesian (resp. standard) basis with

$$\kappa_\pm = \frac{1}{\sqrt{2}}(\mp \kappa_X + i \kappa_Y), \quad \kappa_0 = \kappa_Z. \quad (\text{S7})$$

In this “no-spin” case, the light-shift operator simply describes the displacement of the ground state by the quan-

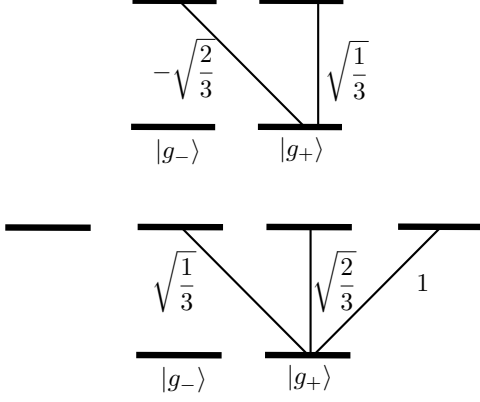


FIG. S1: Amplitude of the couplings for the two components D₁ (top) and D₂ (bottom) of the resonance line of an alkali atom. Here the spin of the nucleus is supposed to be zero. The coupling amplitudes for the g_- state take symmetric values with respect to those indicated for the g_+ state.

tity $|\kappa|^2/\Delta$, where Δ is the detuning of the laser with respect to the atomic transition, $\kappa = (\kappa_X, \kappa_Y, \kappa_Z)$ and

$$|\kappa|^2 = \sum_{\alpha=X,Y,Z} |\kappa_\alpha|^2 = \sum_{m=0,\pm 1} |\kappa_m|^2. \quad (\text{S8})$$

We now take the spin of the valence electron into account, but still assume that the nucleus has spin zero. The ground level is then a two-dimensional manifold (angular momentum $J_g = 1/2$). Because of the fine-structure Hamiltonian, the resonance line of the atom is split into two components D₁ and D₂, corresponding to the transition from the ground state to the excited states with total angular momentum $J_e = 1/2$ and $J_e = 3/2$, respectively.

Let us focus first on the light-shift operator associated with the D₁ transition, which is dominant if the detuning $\Delta_1 = \omega - \omega_1$ of the laser excitation from the D₁ line (frequency ω_1) is much smaller than the detuning Δ_2 from the D₂ line. Using the well-known Clebsch-Gordan coefficients (see *e.g.* Figure S1) and taking Z as quantization axis, we get in the corresponding $\{|g_+\rangle, |g_-\rangle\}$ basis:

$$\hat{V} = \frac{1}{3\Delta_1} \begin{pmatrix} |\kappa_0|^2 + 2|\kappa_-|^2 & -\sqrt{2}(\kappa_0\kappa_-^* + \kappa_+\kappa_0^*) \\ -\sqrt{2}(\kappa_- \kappa_0^* + \kappa_0 \kappa_-^*) & |\kappa_0|^2 + 2|\kappa_+|^2 \end{pmatrix}. \quad (\text{S9})$$

This coupling can be written in a compact form

$$\hat{V} = \frac{|\kappa|^2}{3\Delta_1} \hat{1} + \mathbf{B}_1 \cdot \hat{\mathbf{S}}, \quad (\text{S10})$$

where $\hat{1}$ and $\hat{\mathbf{S}}$ are the identity and spin operators for the spin 1/2 ground state, respectively, and where the (real) effective field \mathbf{B}_1 for the D₁ transition is:

$$\mathbf{B}_1 = -\frac{2i}{3\Delta_1} \kappa \times \kappa^*. \quad (\text{S11})$$

We now take into account both the D₁ and D₂ transitions. A straightforward generalization of the preceding calculation leads to

$$\hat{V} = A \hat{1} + \mathbf{B} \cdot \hat{\mathbf{S}}, \quad (\text{S12})$$

with

$$A = \frac{|\kappa|^2}{3} \left(\frac{1}{\Delta_1} + \frac{2}{\Delta_2} \right) \quad (\text{S13})$$

and

$$\mathbf{B} = \frac{2i}{3} \left(\frac{1}{\Delta_2} - \frac{1}{\Delta_1} \right) \kappa \times \kappa^*. \quad (\text{S14})$$

As a final step we take into account the nucleus spin I . As above we consider the case $I = 3/2$, which leads to a splitting of the ground level into two hyperfine states of angular momentum $F = 1$ and $F = 2$. Here we consider the $F = 1$ state, with the three Zeeman sublevels

$$\begin{aligned} |F = 1, m_F = \pm 1\rangle &= \mp \frac{\sqrt{3}}{2} \left| \mp \frac{1}{2}; \pm \frac{3}{2} \right\rangle \pm \frac{1}{2} \left| \pm \frac{1}{2}; \pm \frac{1}{2} \right\rangle, \\ |F = 1, m_F = 0\rangle &= -\frac{1}{\sqrt{2}} \left| -\frac{1}{2}; \frac{1}{2} \right\rangle + \frac{1}{\sqrt{2}} \left| \frac{1}{2}; -\frac{1}{2} \right\rangle, \end{aligned}$$

where the state $|m_e; m_n\rangle$ is labelled by the quantum numbers for the projection along the Z axis of the electron spin (m_e) and nuclear spin (m_n). We suppose that the detunings Δ_1 and Δ_2 of the laser with respect to the excited states $J_e = 1/2$ and $J_e = 3/2$ are large compared to the hyperfine splittings of these levels. The calculation of the restriction of the coupling (S12) to the $F = 1$ ground level then gives:

$$\hat{V} = A \hat{1} + \mathbf{B}' \cdot \hat{\mathbf{F}}, \quad (\text{S15})$$

where

$$\mathbf{B}' = -\frac{1}{4}\mathbf{B} = \frac{i}{6} \left(\frac{1}{\Delta_1} - \frac{1}{\Delta_2} \right) \kappa \times \kappa^*. \quad (\text{S16})$$

Using (S3) the vector part of the coupling $\hat{U}_{\text{vec}} = \hat{U} - A \hat{1}$ can be written in the Cartesian basis for the $F = 1$ ground state:

$$\hat{U}_{\text{vec}} = i (B'_Z |Y\rangle\langle X| + B'_X |Z\rangle\langle Y| + B'_Y |X\rangle\langle Z|) + \text{H.c.} \quad (\text{S17})$$

HAMILTONIAN FOR RESONANT RAMAN TRANSITIONS

Consider now a scheme such as the one of Fig. S2, where an external field lifts the degeneracy between the three states of the Cartesian basis, and where two monochromatic light waves with the same amplitude (characterized by $\kappa > 0$) and with frequency, phase, wave

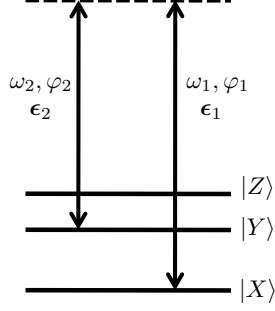


FIG. S2: Laser scheme providing a resonant Raman coupling between two sublevels of the $F = 1$ ground state.

vector and polarizations $\omega_i, \varphi_i, \mathbf{k}_i, \boldsymbol{\epsilon}_i$, $i = 1, 2$ induce a resonant Raman coupling between $|X\rangle$ and $|Y\rangle$.

The transition from $|X\rangle$ to $|Y\rangle$ occurs resonantly via the absorption of a photon in wave 1 and the stimulated emission of a photon in wave 2. Keeping only this resonant process, the relevant contribution to the cross-product $\boldsymbol{\kappa} \times \boldsymbol{\kappa}^*$ entering in (S16) is $\kappa^2 (\boldsymbol{\epsilon}_1 e^{i(\mathbf{k}_1 \cdot \mathbf{r} + \varphi_1)}) \times (\boldsymbol{\epsilon}_2 e^{i(\mathbf{k}_2 \cdot \mathbf{r} + \varphi_2)})^*$, where \mathbf{r} is the position of the atom.

In this work we restrict to waves with linear (real) polarizations in the xy plane, making an angle of $2\pi/3$ with each other. In this case $\boldsymbol{\epsilon}_1 \times \boldsymbol{\epsilon}_2 = (\sqrt{3}/2)\mathbf{u}_z$. The projection of \mathbf{u}_z on each basis vector of the trihedron X, Y, Z is $1/\sqrt{3}$, and the value of B'_Z that is relevant for the resonant coupling between $|X\rangle$ and $|Y\rangle$ (see (S17)) is thus

$$B'_Z = \frac{i\kappa^2}{12} \left(\frac{1}{\Delta_1} - \frac{1}{\Delta_2} \right) e^{i(\mathbf{q}_1 \cdot \mathbf{r} + \varphi_1 - \varphi_2)}, \quad (\text{S18})$$

with $\mathbf{q}_1 = \mathbf{k}_1 - \mathbf{k}_2$. This leads to the resonant part of the vector light-shift operator:

$$\hat{V}_{\text{vec}}^{(\text{res})} = -\Omega e^{i(\mathbf{q}_1 \cdot \mathbf{r} + \varphi_1 - \varphi_2)} |Y\rangle\langle X| + \text{H.c.}, \quad (\text{S19})$$

where we have set

$$\Omega = \frac{\kappa^2}{12} \left(\frac{1}{\Delta_1} - \frac{1}{\Delta_2} \right). \quad (\text{S20})$$

The coupling strength Ω is positive when the laser is tuned between the D_1 and the D_2 lines ($\Delta_1 > 0 > \Delta_2$), and negative otherwise.

Consider for example the case of Rubidium atoms and choose the detuning such that the scalar part of the atom laser coupling (S13) vanishes: $\Delta_2 = -2\Delta_1$, corresponding to the wavelength $\lambda = 790$ nm ($\lambda_1 = 795$ nm, $\lambda_2 = 780$ nm). The optimal two-photon coupling is $\Omega = 3E_R = 9\kappa^2/(2m) \approx 2\pi \times 30$ kHz and the photon scattering rate is $\gamma \approx 9 \times \Gamma\kappa^2/(2\Delta_1^2) \approx 20\text{ s}^{-1}$, where the factor 9 accounts for the number of monochromatic beams shining on the atoms. The time scale for establishing a many-body state such as the Laughlin state can be

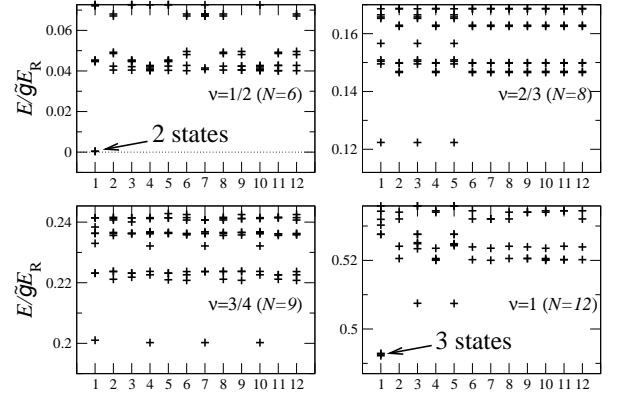


FIG. S3: Low-energy spectra for the OFL with $\Omega/E_R = 3$ in the strong-interaction limit $\tilde{g} \rightarrow \infty$ for a system of size $N_\phi = N_1 N_2 = 6 \times 2$ at filling factors for which the groundstate is incompressible. The crystal momentum $\mathbf{k} \equiv \alpha_1 \mathbf{G}_1/6 + \alpha_2 \mathbf{G}_2/2$ is labelled by the index, $i = 1 + \alpha_1 + 6\alpha_2$ for $\alpha_1 = 0, \dots, 5$ and $\alpha_2 = 0, 1$. The quasi-degenerate groundstates have the expected multiplicities and crystal momenta for the Laughlin state ($\nu = 1/2$), composite fermion states ($\nu = 2/3, 3/4$), and the Moore-Read state ($\nu = 1$).

estimated as the inverse of the corresponding gap $\Delta\mu^{-1}$. Taking $\Delta\mu = 0.02 E_R$ as a typical value (see Fig. 2 of the main text), we obtain $\Delta\mu^{-1} \approx 1$ ms. The heating due to photon scattering should then play a minor role during this time.

ADDITIONAL NUMERICAL RESULTS

We present in this section some additional numerical results alluded to in the main text.

In Fig. S3, we present the excitation spectra for a system of size $N_1 \times N_2 = 6 \times 2$ at all filling factors ($\nu = 1/2, 2/3, 3/4$ and 1) for which we find evidence for incompressible FQH states. These show the expected features of the Laughlin state ($\nu = 1/2$), composite fermion states ($\nu = 2/3, 3/4$) and Moore-Read state ($\nu = 1$) of bosons. On this periodic geometry, these topologically ordered incompressible phases should show groundstate degeneracies (of 2, 3, 4 and 3 respectively) in the thermodynamic limit, separated by an energy gap from the remaining excitations. This is indeed the case, as may be seen clearly in Fig. S3.

In Fig. S4, we present the equivalent excitation spectra for a lowest band formed from states in the lowest Landau level (LLL). As described in the main text, we represent the LLL by the $N_s = 12$ OFL lattice of Ref. 3, the lowest band of which has properties that are indistinguishable from those of the LLL for a lattice coupling of $\Omega' = 10E_R$. This very close equivalence arises from the very rapid convergence of the properties of the N_s -state OFL lattice of Ref. 3 to those of a charged particle in a uniform magnetic field, the spatial fluctuations of

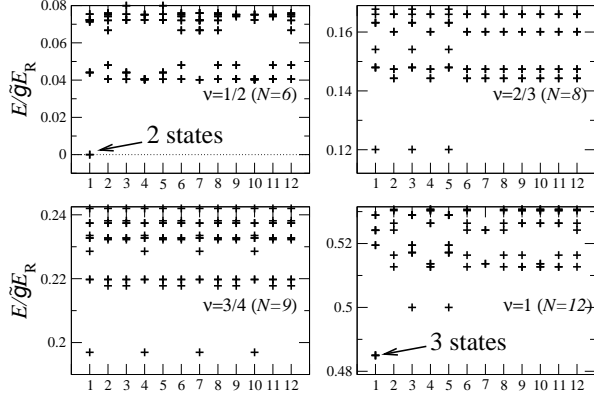


FIG. S4: Low-energy spectra for contact-interacting bosons in the LLL for a system of the same size and geometry as Fig. S3 ($N_\phi = 12$), at filling factors $\nu = 1/2, 2/3, 3/4, 1$ for which the groundstate is incompressible. The crystal momentum is labelled as for Fig. S3.

the energy and effective magnetic field experienced by the lowest energy dressed state of the OFL falling exponentially with increasing N_s , and already negligible for $N_s = 12$ [3]. Interpolation between the $N_s = 3$ OFL of this paper and the LLL leads to a smooth evolution both of the single-particle levels of the lowest bands, and of the many body spectrum for bosons occupying this lowest band. This establishes that the FQH phases of these two systems are the same. Moreover, the spectra of the OFL (Fig. S3) differ only very slightly from those of the LLL (Fig. S4). The main qualitative difference is that some approximate degeneracies in Fig. S3 become exact degeneracies connected to the many-body translational symmetry of the LLL [4]. Furthermore, the approximate 3-fold groundstate degeneracy of Fig. S3(d) becomes an exact degeneracy in the LLL Fig. S4(d). This is due to a $\pi/3$ rotational symmetry of the LLL in this geometry of $N_1 \times N_2 = 6 \times 2$ (for which the sides of the simulation cell have equal length $|\mathbf{L}_1| = |\mathbf{L}_2|$), which transforms the three groundstates of the Moore-Read state in the LLL

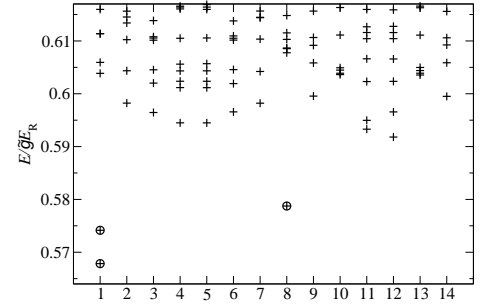


FIG. S5: Low-energy spectrum for the OFL with $\Omega/E_R = 3$ in the strong-interaction limit $\tilde{g} \rightarrow \infty$ for a system of size $N_\phi = N_1N_2 = 7 \times 2$ at filling factor $\nu = 1$. The crystal momentum $\mathbf{k} \equiv \alpha_1 \mathbf{G}_1/7 + \alpha_2 \mathbf{G}_2/2$ is labelled by the index, $i = 1 + \alpha_1 + 7\alpha_2$ for $\alpha_1 = 0, \dots, 6$ and $\alpha_2 = 0, 1$. The three quasi-degenerate groundstates (marked by circles) are at the expected crystal momenta for the Moore-Read state. No symmetry protects these quasi-degenerate levels. The same quasi-degeneracy appears for contact interacting bosons in the LLL [5].

into each other. We emphasize that, in general, this three-fold quasi-degeneracy is unrelated to any symmetry, but is an emergent quasi-degeneracy in the thermodynamic limit. This is evidenced by studies on other system sizes and geometries, just as in the LLL [5]. For example, Fig. S5 shows the spectrum for the OFL for $N = 14$ particles in a system of size $N_1 \times N_2 = 7 \times 2$ for which no symmetry relates the three quasi-degenerate groundstates.

-
- [1] F. Gerbier *et al.*, Phys. Rev. A **73**, 041602 (2006).
 - [2] C. Cohen-Tannoudji and J. Dupont-Roc, Phys. Rev. A **5**, 968 (1972).
 - [3] N. R. Cooper and R. Moessner, Phys. Rev. Lett. **109**, 215302 (2012).
 - [4] F. D. M. Haldane, Phys. Rev. Lett. **55**, 2095 (1985).
 - [5] N. R. Cooper, Advances in Physics **57**, 539 (2008).